NACA RM L50A27

NACA

RESEARCH MEMORANDUM

THE EFFECT OF SPANWISE AILERON LOCATION ON THE ROLLING EFFECTIVENESS OF WINGS WITH 0° AND 45° SWEEP AT SUBSONIC, TRANSONIC, AND SUPERSONIC SPEEDS

By H. Kurt Strass

Langley Aeronautical Laboratory
Langley Air Force Base, Va.

NATIONAL ADVISORY COMMITTEE
FOR AERONAUTICS

WASHINGTON
April 25, 1950

NATIONAL ADVISORY COMMITTEE FOR AERONAUTICS

RESEARCH MEMORANDUM

THE EFFECT OF SPANWISE AILERON LOCATION ON THE ROLLING EFFECTIVENESS OF WINGS WITH 0° AND 45° SWEEP AT SUBSONIC, TRANSONIC, AND SUPERSONIC SPEEDS

By H. Kurt Strass

SUMMARY

The effect of spanwise aileron location on the rolling effectiveness of 0.2-chord plain faired ailerons on untapered wing plan forms having 0° and 45° sweep, NACA 65A009 airfoil sections, and an aspect ratio of 3.7 has been investigated at subsonic, transonic, and supersonic speeds by the Langley Pilotless Aircraft Research Division utilizing rocket-propelled test vehicles. In addition, drag data are presented for all the configurations discussed in this investigation.

The results show that, for unswept wings, there was little or no change in the rolling effectiveness with spanwise aileron location of the particular aileron configuration tested when the effects of control area and moment arm were taken into consideration. However, spanwise control location on wings of 45° sweep is an extremely important consideration inasmuch as the inboard half-span aileron was much more effective than the outboard half-span aileron throughout the entire speed range tested and proportionally more effective than the full-span aileron when the effects of control area and moment arm were taken into consideration. The inboard aileron contributed about 60 percent of the full-span effectiveness at a Mach number of 0.7 with the proportion continually increasing until at a Mach number of 1.5 and higher, the inboard aileron was almost as effective as the full-span configuration.

In addition, data are presented for a shielded horn balance attached to the outboard half-span aileron configuration for both the swept and unswept cases. Little change in rolling performance was observed.

INTRODUCTION

In continuance of a general investigation of wing-aileron rolling effectiveness being conducted by the Langley Pilotless Aircraft Research Division utilizing rocket-propelled test vehicles in free flight at subsonic, transonic, and supersonic speeds, a limited investigation of the effects of spanwise aileron location on rolling effectiveness has been completed. The purpose of these tests was to determine the relative effectiveness of inboard and outboard plain ailerons in the subsonic, transonic, and supersonic regions. Two wing plan forms were employed: One was unswept with the ailerons at the inboard half-span, the outboard half-span, and the full-span location; the other plan form used the same aileron locations but the wing was swept back 45°. Some effects of varying the wing torsional rigidity are also presented. In addition, relatively large shielded horn balances were attached to the outer half-span aileron on both the swept and unswept wings to determine the effects of this type of control upon the rolling effectiveness and the drag.

SYMBOLS

A	aspect ratio $\left(\frac{b^2}{S}\right)$, 3.7
b	diameter of circle swept by wing tips (with regard to rolling characteristics, this diameter is considered to be the effective span of the three-fin models), 2.18 feet
c	wing chord parallel to model center line, 0.59 foot
C_{D_T}	drag coefficient based on total exposed wing area of 1.56 square feet
M	Mach number
m	concentrated couple, applied near wing tip in a plane parallel to free stream and normal to wing-chord plane, inch-pounds
p	rolling velocity, radians per second
$\frac{pb}{2V}$	wing-tip helix angle, radians
R	Reynolds number based on wing chord parallel to model center line

S	area of two wing panels measured to fuselage center line, 1.29 square feet
V	flight-path velocity, feet per second
C_{l_p}	rate of change of rolling-moment coefficient with wing-tip helix angle
δ_a	deflection of each aileron measured in plane perpendicular to chord plane and parallel to model center line (average for three wings), degrees
λ	taper ratio of tip chord to root chord at model center line
Λ	angle of sweep, degrees
i_w	average wing incidence for three wings measured in plane of δ_a, positive when tending to produce clockwise roll as seen from rear, degrees
θ	angle of wing twist, produced by m, at any section along wing span in a plane parallel to free stream and normal to wing-chord plane, radians
$\left(\frac{\theta}{m}\right)_r$	wing-torsional-stiffness parameter measured at aileron midspan parallel to free stream, radians per inch-pound

MODELS AND TESTS

The test vehicles used in the present investigation are described in figures 1 to 4. The exposed wing area was 1.56 square feet, the area of two wings taken to the center line of the fuselage was 1.29 square feet, the aspect ratio was 3.7, and the airfoil section was the NACA 65A009. The ailerons were of 0.2 chord and simulated sealed ailerons with no surface discontinuity at the aileron hinge axis. Two wing plan forms were employed: One was unswept with the ailerons at the exposed inboard half-span, outboard half-span, and full-span location; the other plan form used the same aileron locations but the wing was swept back 45°. A cross section of the horn balance is presented in figure 4.

The test vehicles were launched at the Langley Pilotless Aircraft Research Station, Wallops Island, Va. The test vehicles were propelled by a two-stage rocket propulsion system to a Mach number of about 1.8. During a 10-second period of coasting flight following rocket-motor

burnout, time histories of the rolling velocity were obtained with special radio equipment and the flight-path velocity was obtained by the use of CW Doppler radar. These data, in conjunction with atmospheric data obtained with radiosondes, permit the evaluation of the aileron rolling effectiveness in terms of the parameter $pb/2V$ as a function of Mach number. In addition, the variation of drag coefficient with Mach number was obtained by a method involving the differentiation of the curve of flight-path velocity against time for power-off flight. The average variation in Reynolds number with Mach number for the tests reported in this paper is presented in figure 5. The technique is described more fully in references 1 and 2.

ACCURACY

Based upon previous experience the experimental accuracy is estimated to be within the following limits:

$\frac{pb}{2V}$ (due to limits on model constructional accuracy)	±0.005
$\frac{pb}{2V}$ (due to limitations on instrumentation)	±0.0005
C_{D_T} (at subsonic speeds)	±0.003
C_{D_T} (at supersonic speeds)	±0.002
M	±0.01
i_w (departure from measured values), degrees	±0.10
δ_a (departure from measured values), degrees	±0.25

Figure 6 shows the typical effect of the moment of inertia about the roll axis on the measured variation of $pb/2V$ with Mach number. The correction was made by applying the method described in reference 1 and by using an arbitrarily estimated value of $C_{l_p} = -0.2$ for the damping-in-roll derivative over the entire Mach number range. This value for the damping coefficient was chosen to show that, for any reasonable value, the magnitude of the correction is small. The data used in this paper have not been corrected for inertia effects.

The measured values of $pb/2V$ have been corrected to values corresponding to $i_w = 0^\circ$ and $\delta_a = 5^\circ$. The correction for incidence, which was determined experimentally by means of test vehicles identical to those of the present tests except that the ailerons were undeflected and the wings set at small values of incidence, is given by the following relation:

$$\Delta\frac{pb}{2V} = \frac{1.5i_w}{57.3} = 0.0262i_w$$

The correction for aileron deflection was made by dividing the measured value of $pb/2V$ by the actual aileron deflection and then multiplying by 5.

RESULTS AND DISCUSSION

The effect of spanwise location on the rolling characteristics of plain, sealed, 0.2-chord, trailing-edge ailerons is presented in figures 7 to 12, for both unswept wings and wings of 45° sweep, as curves of $pb/2V$ and C_D plotted against Mach number. In addition, drag data are included as a matter of interest to illustrate the relation between transonic drag rise and control effectiveness. The data are presented first as separate plots for duplicate models of each configuration in order to show the degree of accuracy obtained with supposedly identical models. It will be noted in figure 8 that there is a disagreement between the two flights as far as the absolute magnitude of $pb/2V$ is concerned. As this difference is in the form of an almost constant increment of 0.01 in the value of $pb/2V$ rather than a change in the shape of the curves, it is believed that a probable explanation of the displacement could be a differential error in wing incidence of approximately 0.38° or an equivalent amount of wing twist. In general, uncorrected data from duplicate models agree more closely than the results presented in figure 8.

In figure 13 are summarized the results for all the configurations tested. The rolling effectiveness parameter has been corrected to $i_w = 0°$ and $\delta_a = 5°$ and, for those configurations for which results were obtained with more than one nominally identical model, the results have been averaged. From examination of the summary plot, it is apparent that if consideration is made for the effects of area and moment arm the variation of aileron effectiveness with Mach number for the unswept wing plan forms is substantially the same for all three configurations. In the region between $M = 0.85$ and $M = 0.95$, all three configurations exhibited an abrupt decrease in effectiveness at the same Mach number. The full-span aileron on the swept plan form exhibited a smooth transition from the subsonic to the supersonic range but the partial-span ailerons on the same plan form showed a small discontinuity between $M = 0.85$ and $M = 1.00$. Although a comparison of the rolling effectiveness of the inboard and outboard ailerons for the unswept wing agreed with previous experience in that the inner half-span aileron was less effective than the outer half-span, a similar comparison for the 45° sweptback wing showed the inboard aileron to be more effective. The outboard aileron on the swept wing had less rolling effectiveness than the inboard although the moment arm for the outboard

aileron was approximately twice as large as the inboard. The inboard aileron contributed about 60 percent of the full-span effectiveness at a Mach number of 0.7 with the proportion continually increasing until at a Mach number of 1.5 and higher the inboard location was almost as effective as the full-span configuration. Note that the outboard aileron maintained relatively good rolling effectiveness at the highest speeds. Included in figure 13 are estimated values of $pb/2V$ obtained by using the data presented in reference 3 and the values of C_{l_p} given in reference 4. The values of C_{l_p} were corrected for the slope of the lift curve of the airfoil section used on the test vehicles. This slope was estimated to be 95 percent of the theoretical lift-curve slope. The values presented are calculated for $M \rightarrow 0$ and predict the relative control effectiveness of the controls on the unswept wings but do not appear adequate for swept wings at the speeds investigated.

The unusually low rolling effectiveness of the outer half-span aileron as compared to the inner half-span aileron on the sweptback wing appears to be primarily an aerodynamic effect peculiar to that configuration rather than a loss of control due to wing twisting, based upon the results of two models which were included in the test program to verify this phenomenon. The wing panels of the outer half-span check model were made approximately twice as stiff in twist as the wing panels of the basic models, and the wing panels of the inner half-span check model were made approximately three-quarters as rigid in twist as the basic models, thereby accentuating the comparison between the two aileron locations. From examination of the results presented in figure 14, it is evident that the relative loss in control effectiveness due to structural deformation is small. This does not mean to imply that there was no loss of effectiveness with increasing Mach number or decreasing stiffness. According to references 5 and 6, the loss of effectivenesss due to wing twisting at $M = 1.8$ was approximately 25 percent for the unswept models of identical construction. (See figure 15.) Unpublished data indicate that unswept and sweptback models of equal torsional rigidity experience approximately the same relative loss of control effectiveness at a given Mach number.

As a matter of interest some information on the effect of adding a shielded horn balance to the outer half-span configurations is presented in figures 16 to 18. Figures 16 and 17 show the data obtained from duplicate models. In figure 18, averaged values taken from the two preceding figures are compared with the plain aileron configurations from figure 13. The addition of the shielded horn balance apparently had no appreciable effect upon the performance of the plain aileron in the supersonic region although a slight decrease in the magnitude of the rolling effectiveness is apparent for the unswept configuration in the region below $M = 0.85$. The drag was slightly higher for both of the horn-balance ailerons.

CONCLUSIONS

An investigation to determine the effect of spanwise aileron location on the rolling effectiveness of wings with 0° and 45° sweep at subsonic, transonic, and supersonic speeds indicated the following conclusions:

1. Spanwise aileron location appears to have little effect on the effectiveness of an 0.2-chord plain faired aileron on an unswept wing plan form when allowance is made for the effect of the area and moment arm of the control.

2. Spanwise aileron location on wings of 45° sweep is extremely critical. The inboard half-span aileron was much more effective than the outboard half-span aileron throughout the entire speed range tested and about 60 percent as effective as the full-span aileron at a Mach number of 0.7 with the proportion continually increasing with increasing Mach number until at a Mach number of 1.5 the inboard aileron was almost as effective as the full-span aileron.

3. The addition of a horn balance to the outer half-span plain aileron configurations caused little change in the rolling effectiveness of the control.

Langley Aeronautical Laboratory
National Advisory Committee for Aeronautics
Langley Air Force Base, Va.

REFERENCES

1. Sandahl, Carl A., and Marino, Alfred A.: Free-Flight Investigation of Control Effectiveness of Full-Span 0.2-Chord Plain Ailerons at High Subsonic, Transonic, and Supersonic Speeds to Determine Some Effects of Section Thickness and Wing Sweepback. NACA RM L7D02, 1947.

2. Sandahl, Carl A.: Free-Flight Investigation of Control Effectiveness of Full-Span, 0.2-Chord Plain Ailerons at High Subsonic, Transonic, and Supersonic Speeds to Determine Some Effects of Wing Sweepback, Taper, Aspect Ratio, and Section Thickness Ratio. NACA RM L7F30, 1947.

3. Lowry, John G., and Schneiter, Leslie E.: Estimation of Effectiveness of Flap-Type Controls on Sweptback Wings. NACA TN 1674, 1948.

4. Bird, John D.: Some Theoretical Low-Speed Span Loading Characteristics of Swept Wings in Roll and Sideslip. NACA TN 1839, 1949.

5. Tucker, Warren A., and Nelson, Robert L.: Theoretical Characteristics in Supersonic Flow of Constant-Chord Partial-Span Control Surfaces on Rectangular Wings Having Finite Thickness. NACA TN 1708, 1948.

6. Tucker, Warren A., and Nelson, Robert L.: The Effect of Torsional Flexibility on the Rolling Characteristics at Supersonic Speeds of Tapered Unswept Wings. NACA TN 1890, 1949.

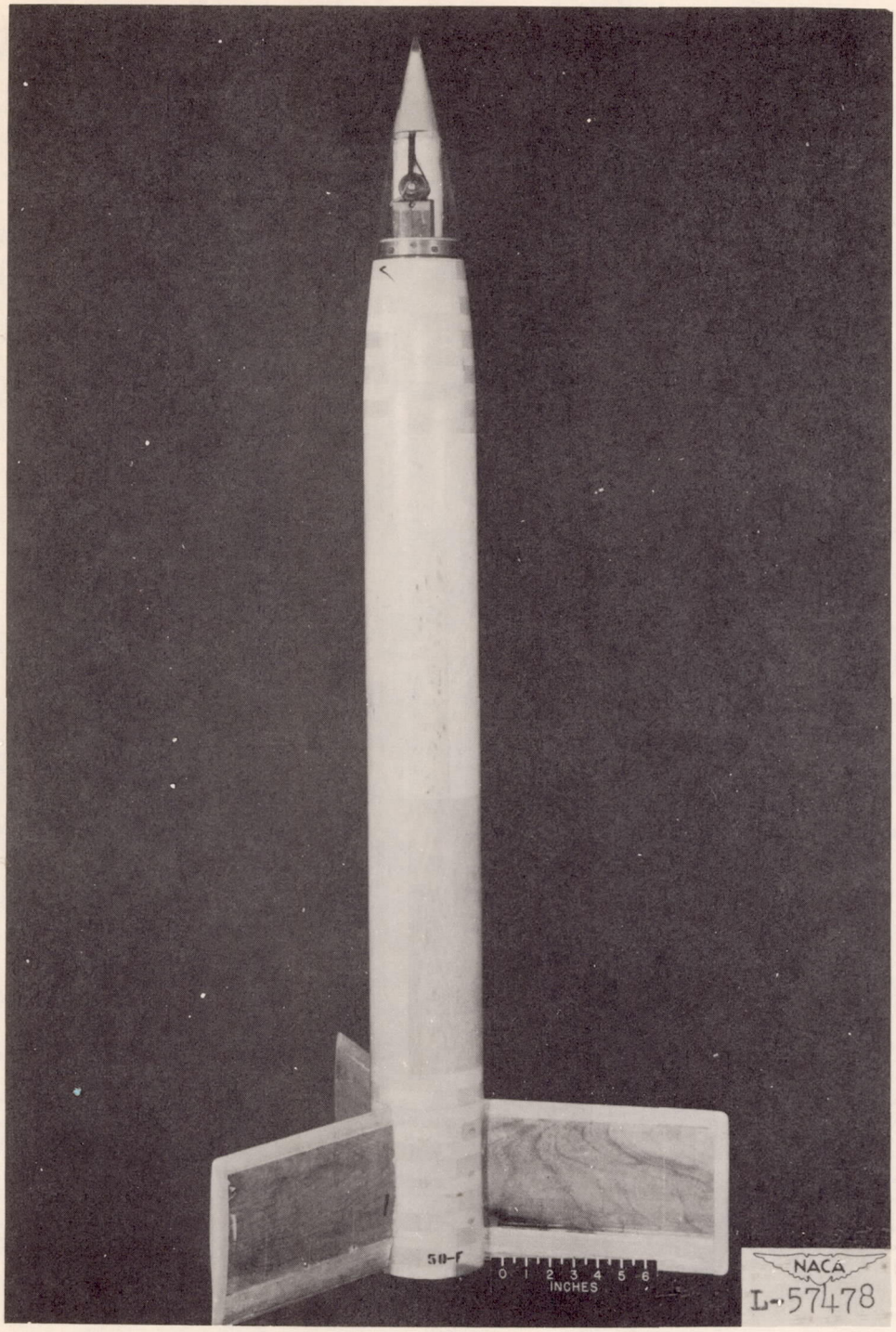

Figure 1.- Typical test vehicle.

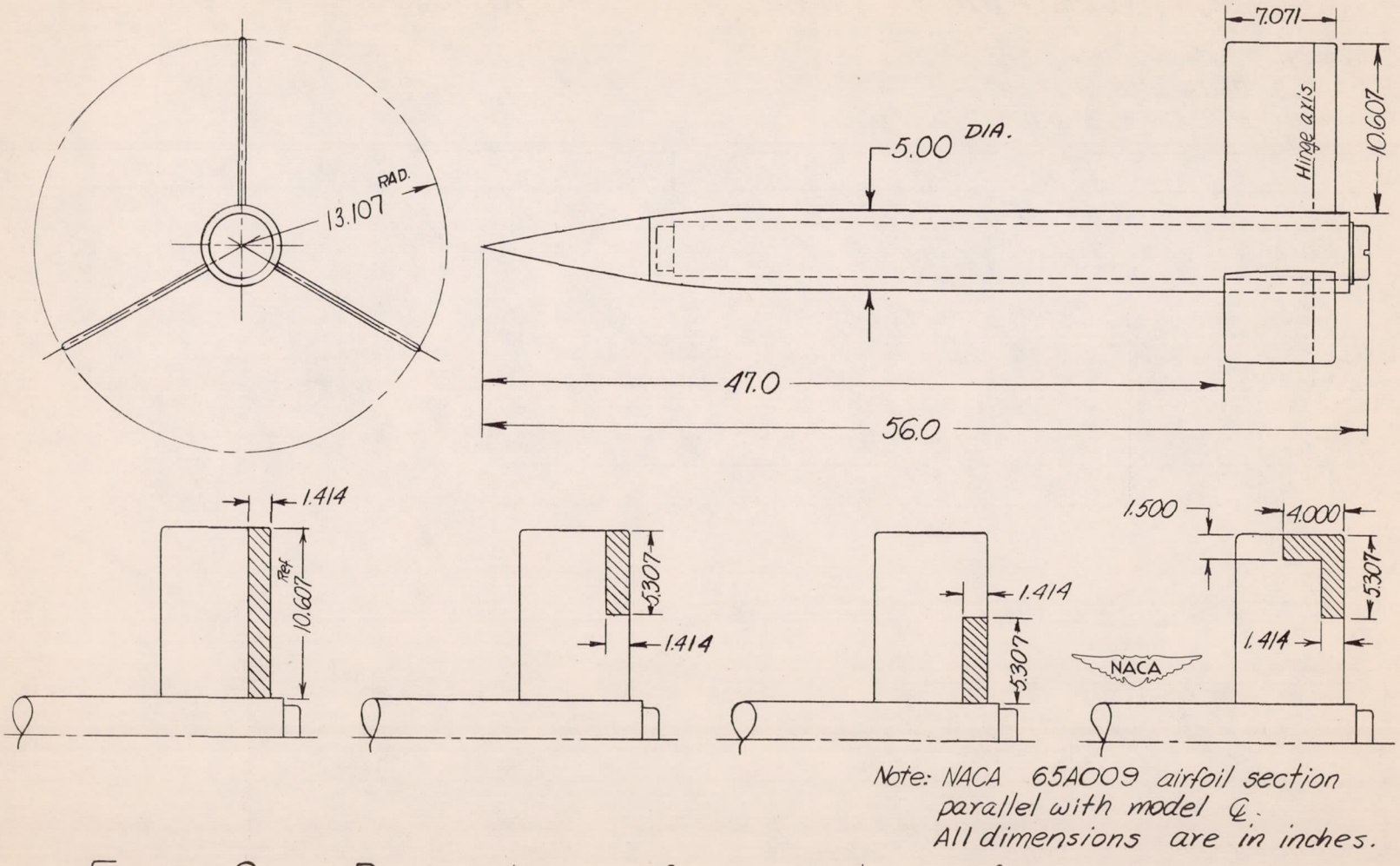

Figure 2. -Description of unswept configurations.

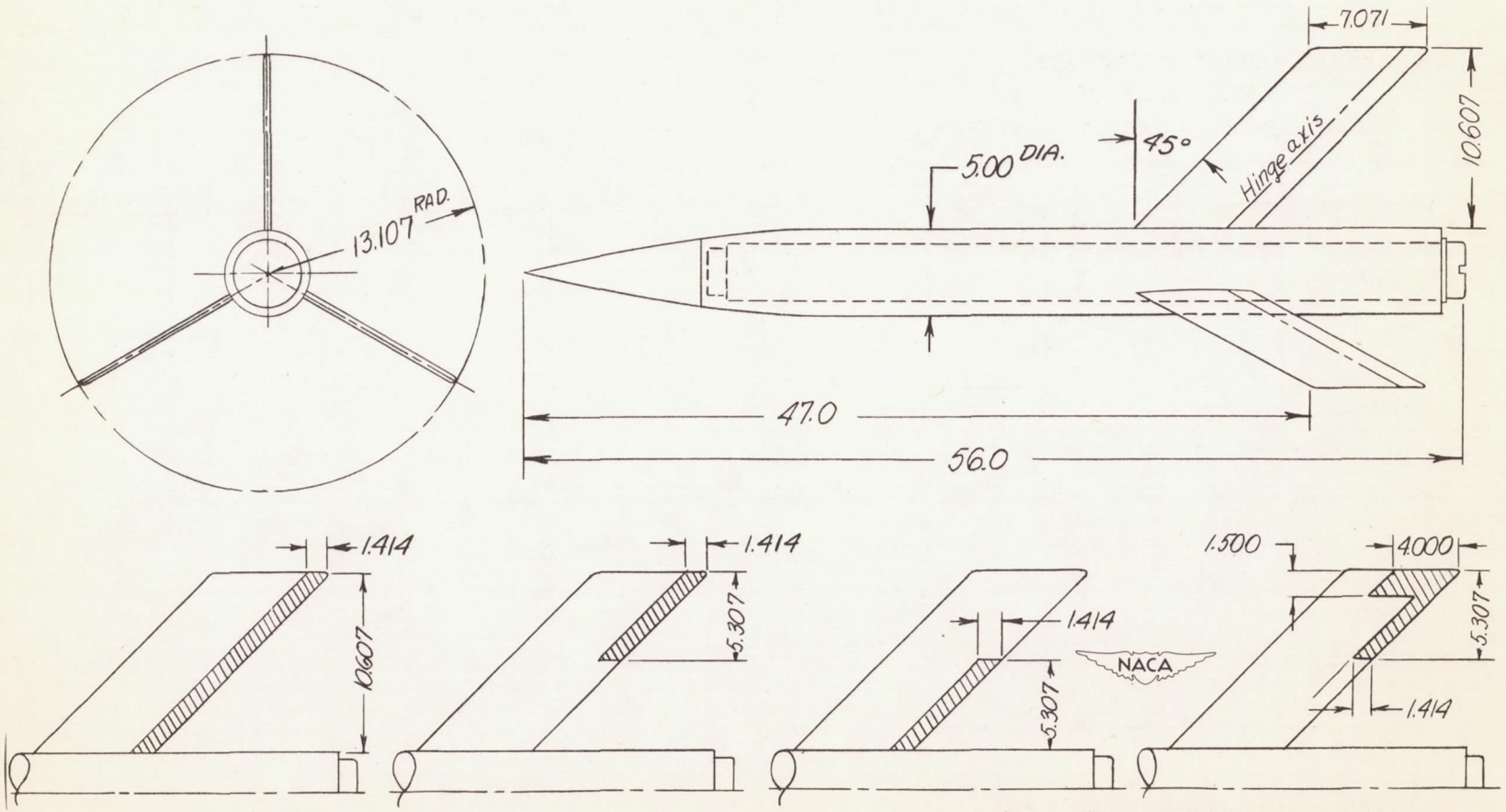

Note: NACA 65A009 airfoil section parallel with model ℄.
All dimensions are in inches.

Figure 3. - Description of swept configurations.

Aileron Coordinates, inches

X	Y	X	Y
0	0	0.648	0.130
0.030	0.040	.805	.134
.058	.055	.995	.135
.115	.075	1.230	.133
.183	.090	1.520	.128
.260	.104	1.740	.120
.360	.115	2.223	.098
.500	.125	2.595*	.082

* Straight sides beyond this point

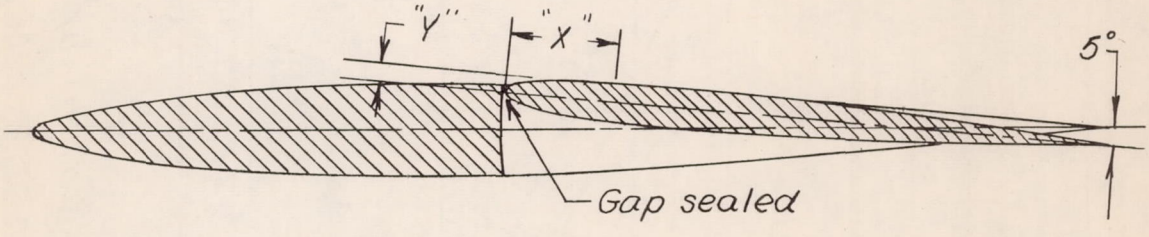

Figure 4.- Typical section through wing tip illustrating contour of horn balance.

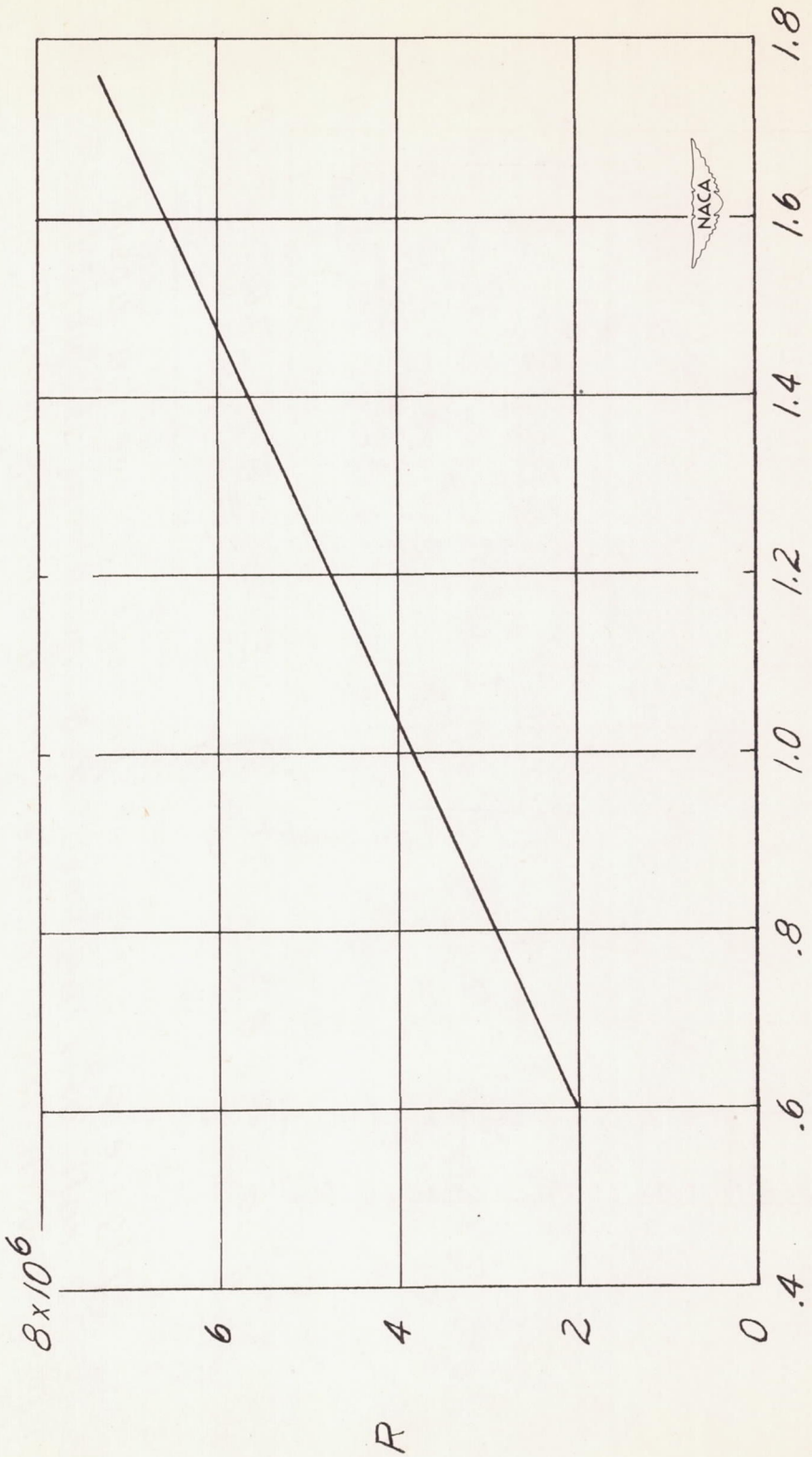

Figure 5.- Average variation of Reynolds number with Mach number.

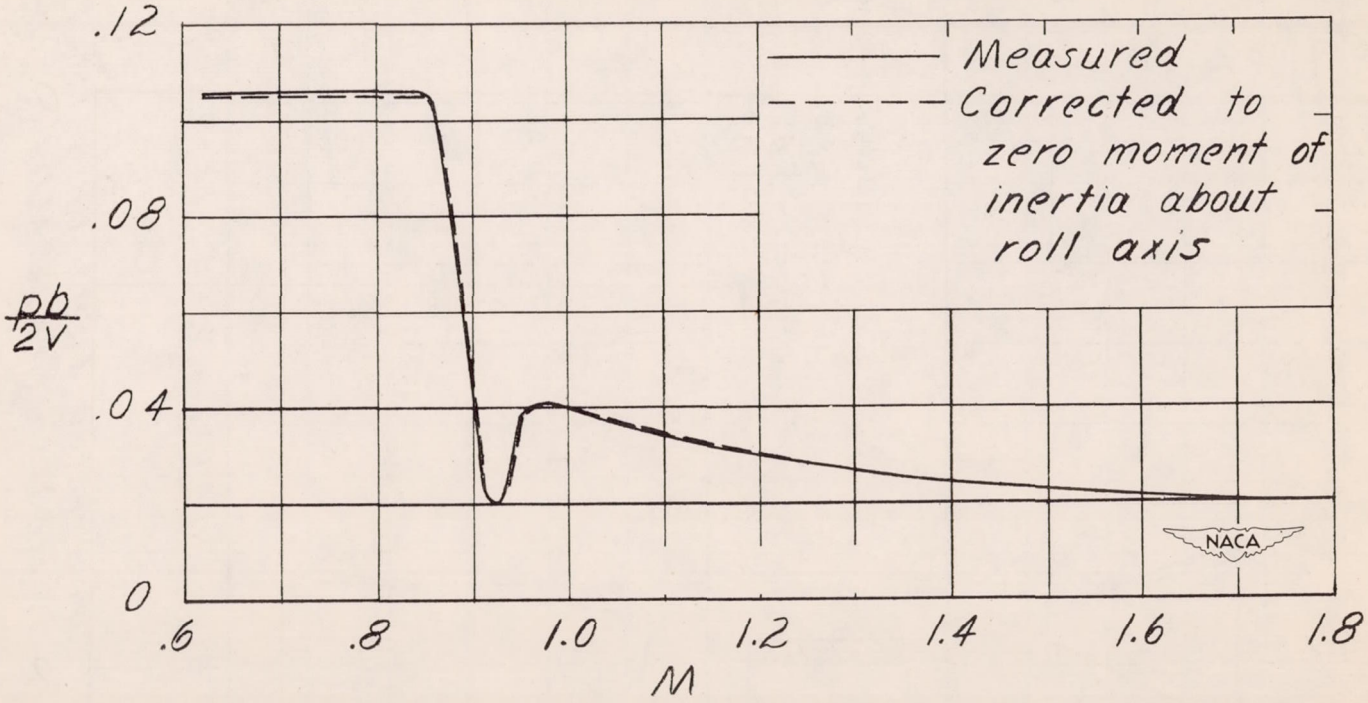

Figure 6.- Effect of moment of inertia about roll axis on measured variation of pb/2V with Mach number for a typical model.

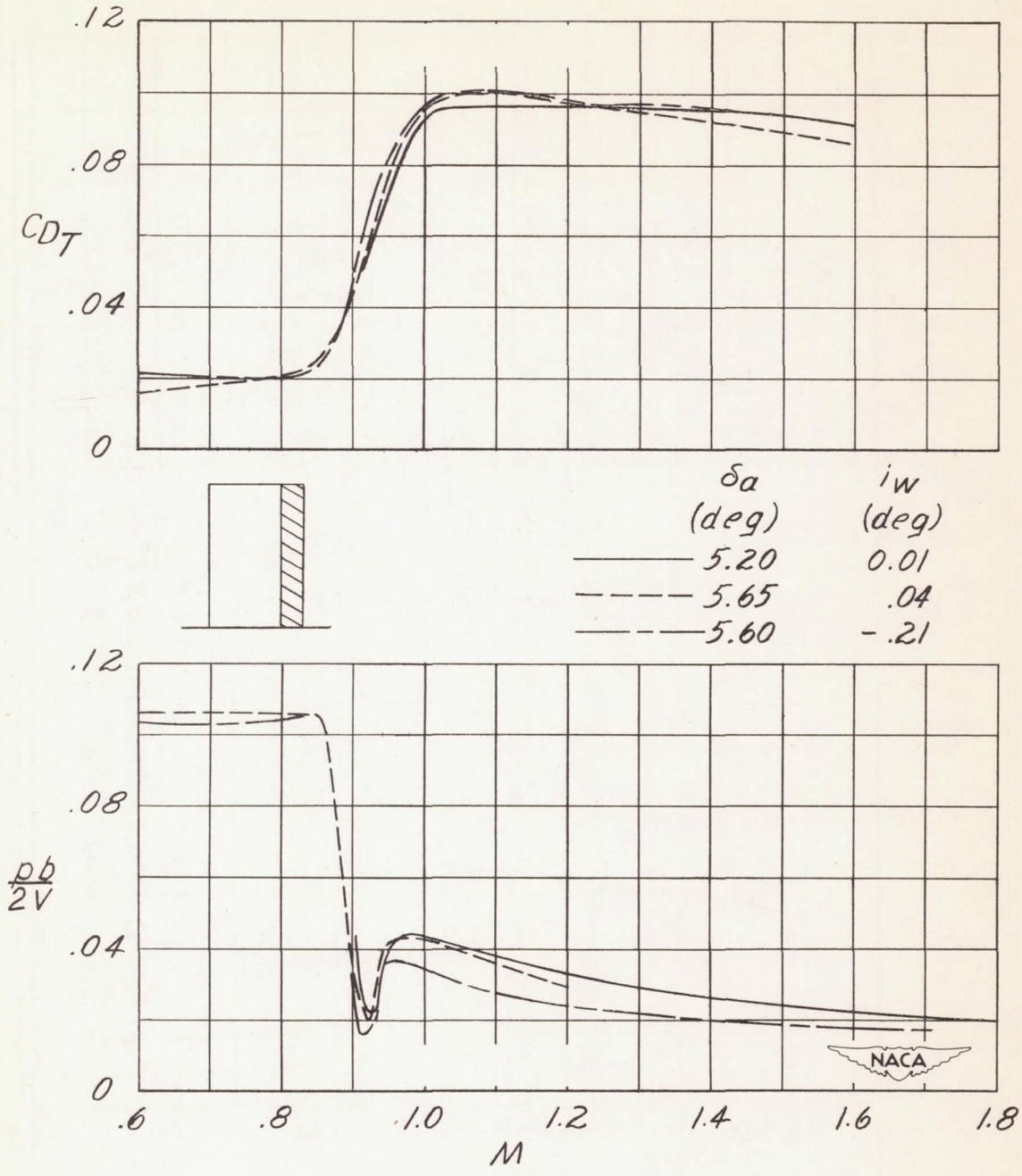

Figure 7.- Uncorrected flight data for full-span aileron. Airfoil section 65A009; $\Lambda = 0°$; $A = 3.7$.

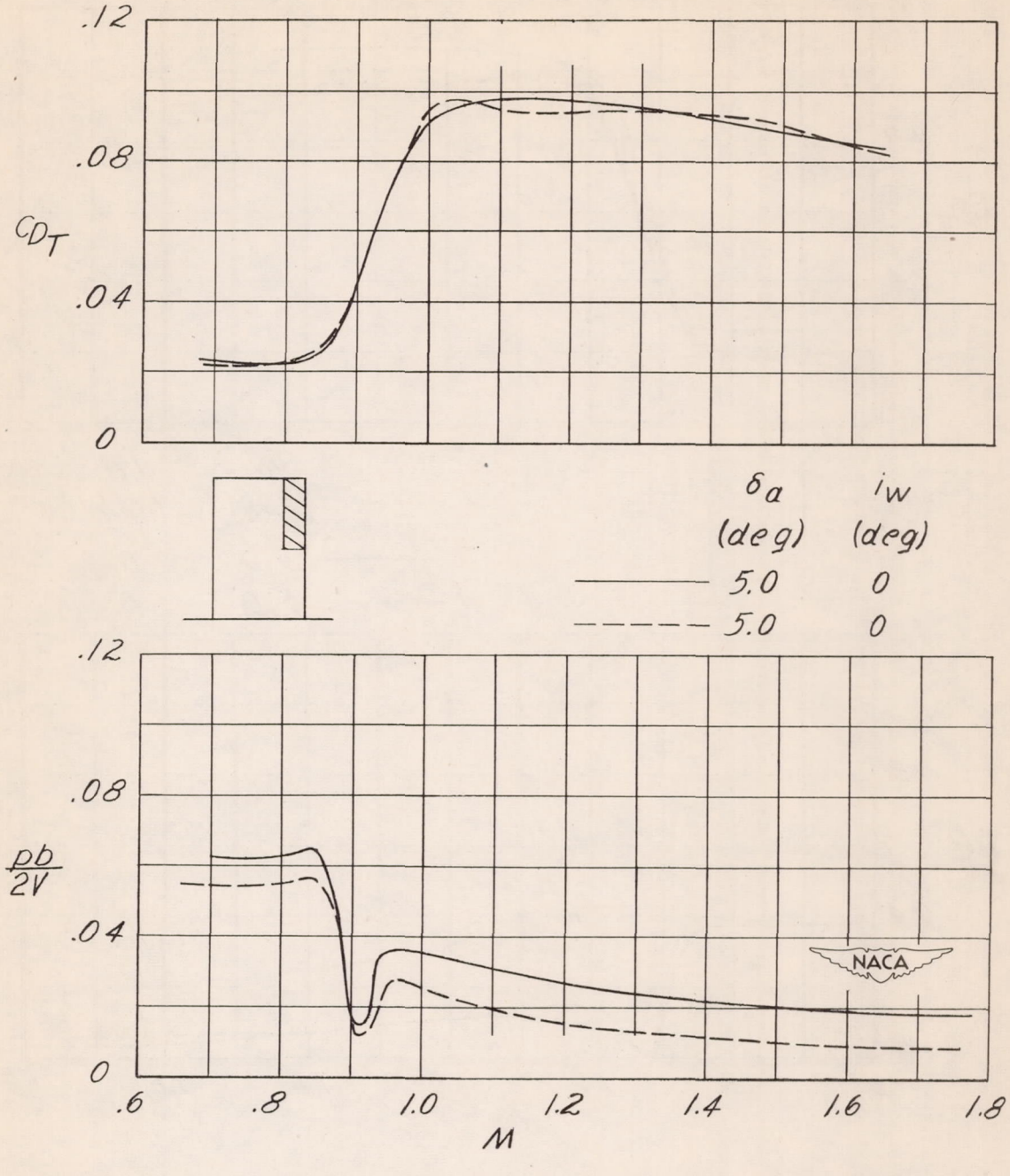

Figure 8.- Uncorrected flight data for outboard aileron. Airfoil section 65A009; $\Lambda = 0°$; $A = 3.7$.

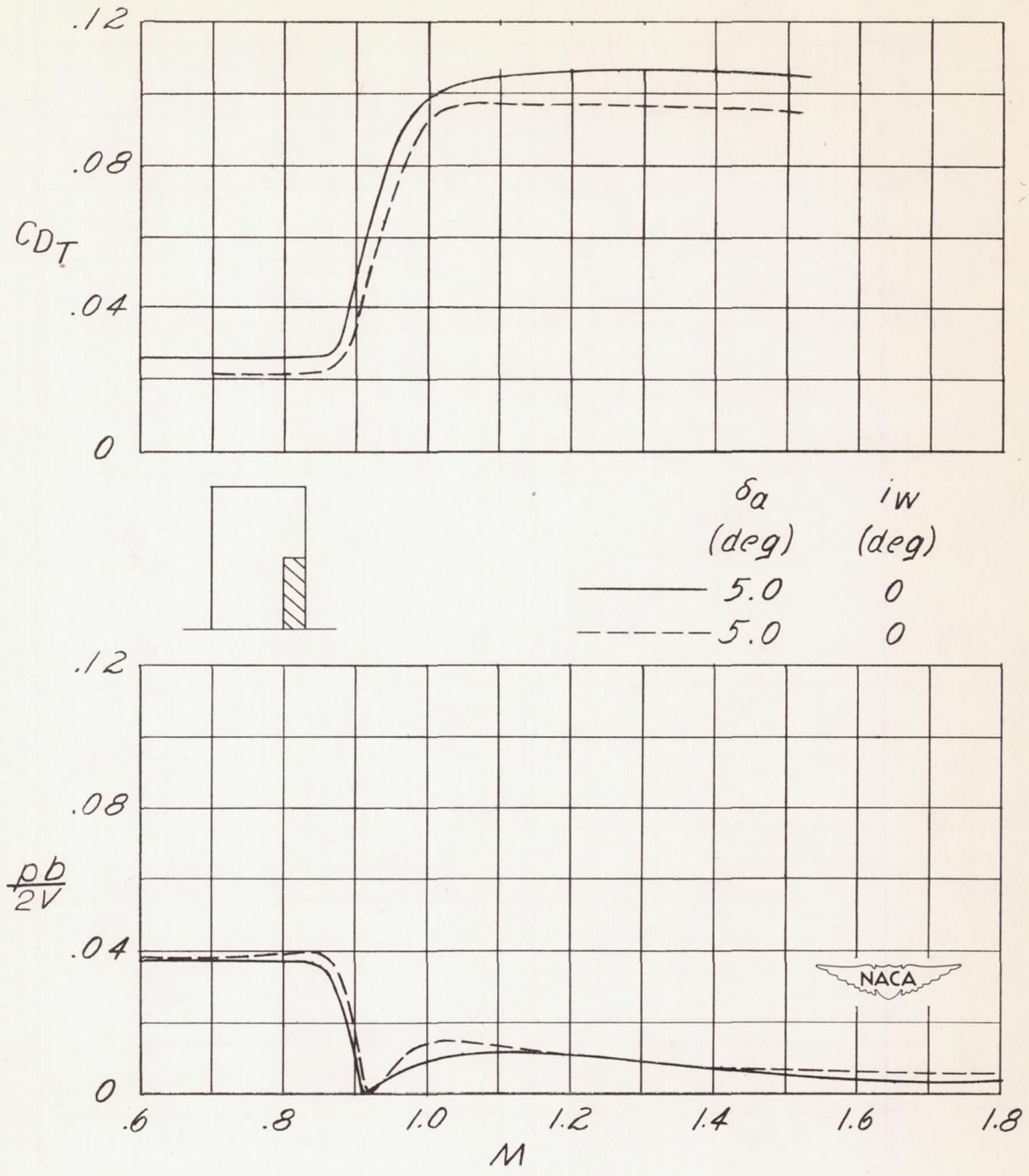

Figure 9.-Uncorrected flight data for inboard aileron. Airfoil section 65A009; $\Lambda = 0°$; $A = 3.7$

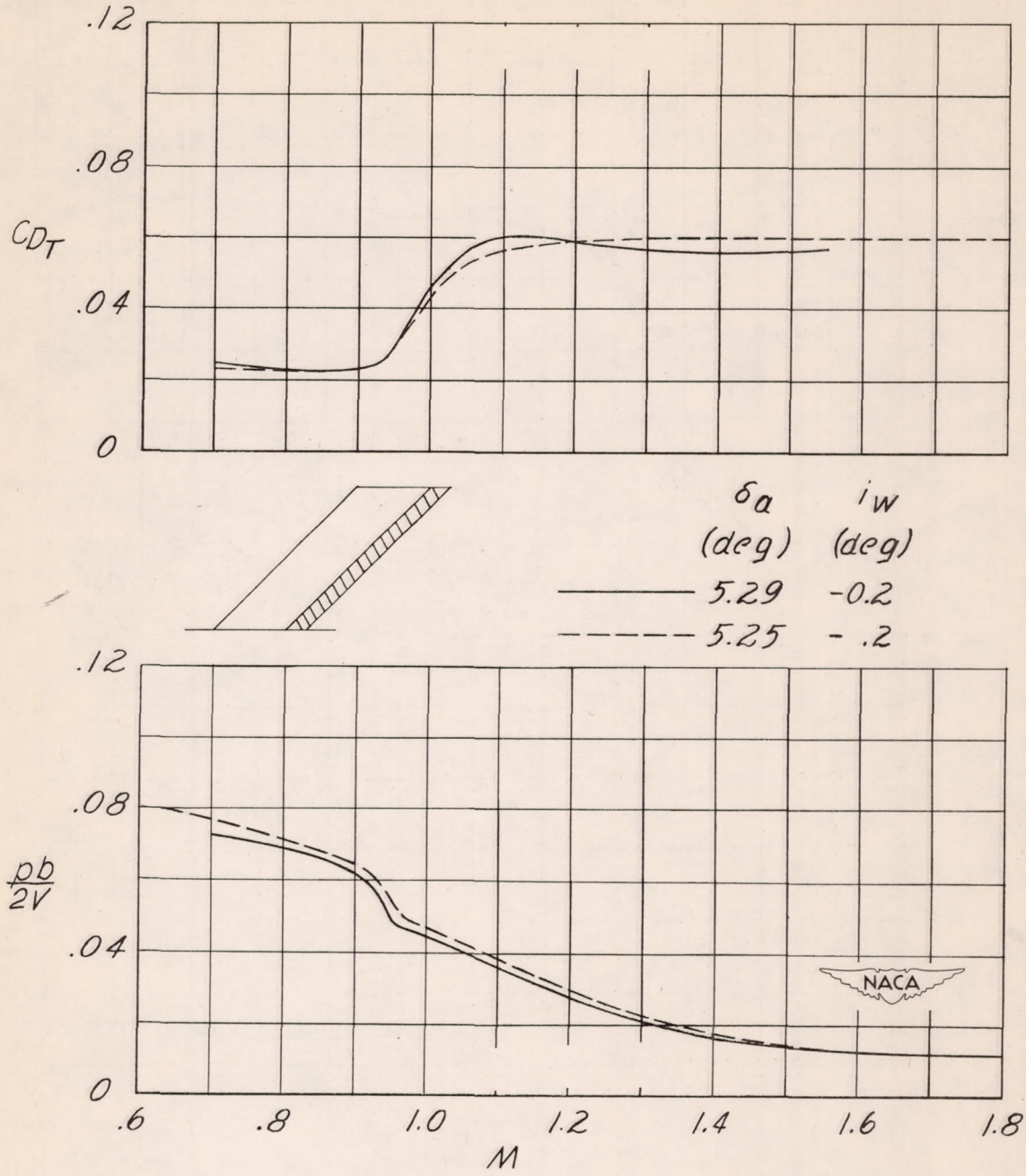

Figure 10. - Uncorrected flight data for full-span aileron. Airfoil section 65A009; $\Lambda = 45°$; $A = 3.7$.

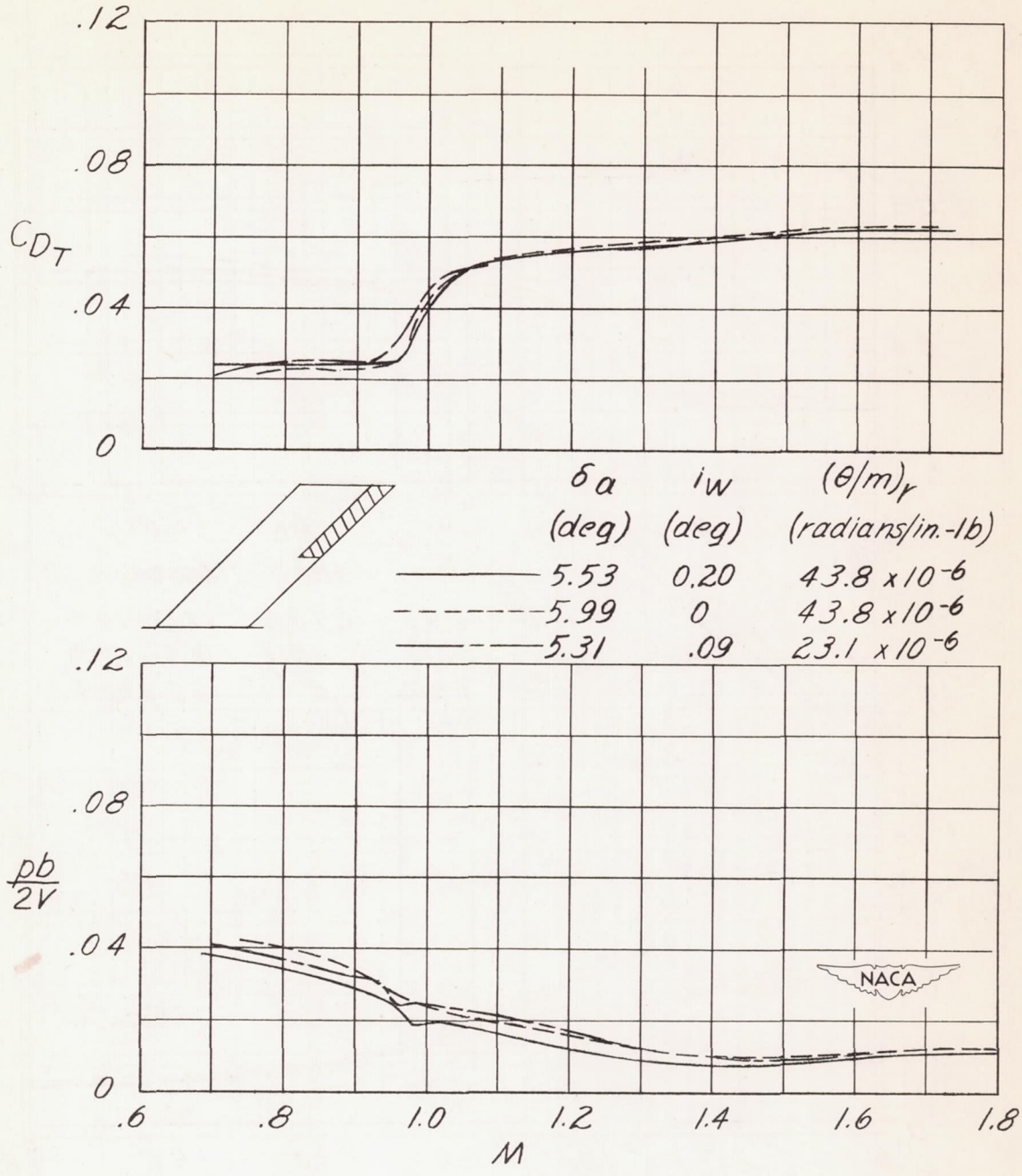

Figure 11.- Uncorrected flight data for outboard aileron. Airfoil section 65A009; $\Lambda = 45°$; $A = 3.7$.

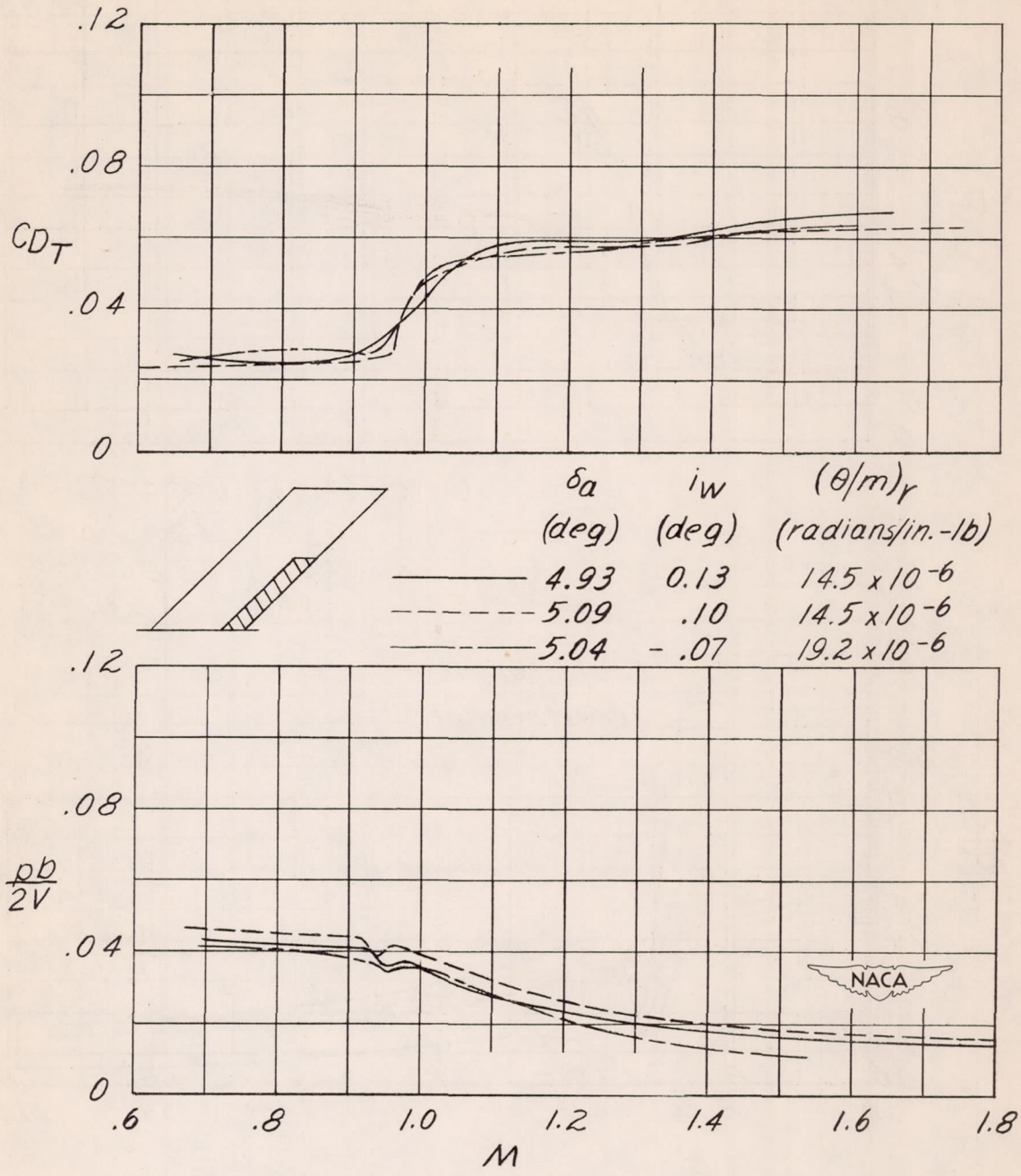

Figure 12.- Uncorrected flight data for inboard aileron. Airfoil section 65A009; $\Lambda = 45°$; $A = 3.7$.

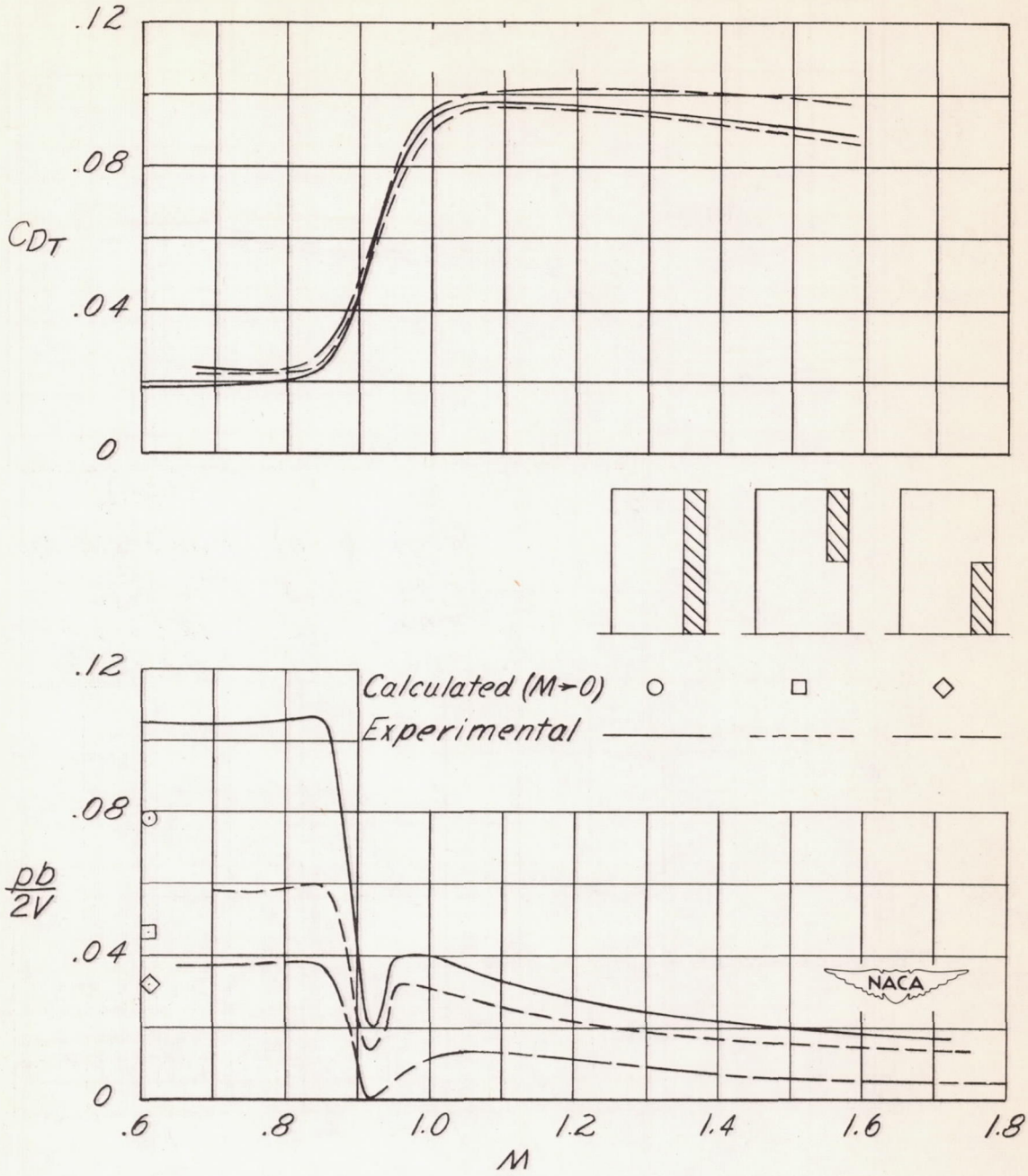

(a) $\Lambda = 0°$; $\delta_a = 5°$.

Figure 13.- Effect of aileron location on the variation of $pb/2V$ and C_{D_T} with Mach number. Airfoil section 65A009; $\lambda = 1.0$; $A = 3.7$.

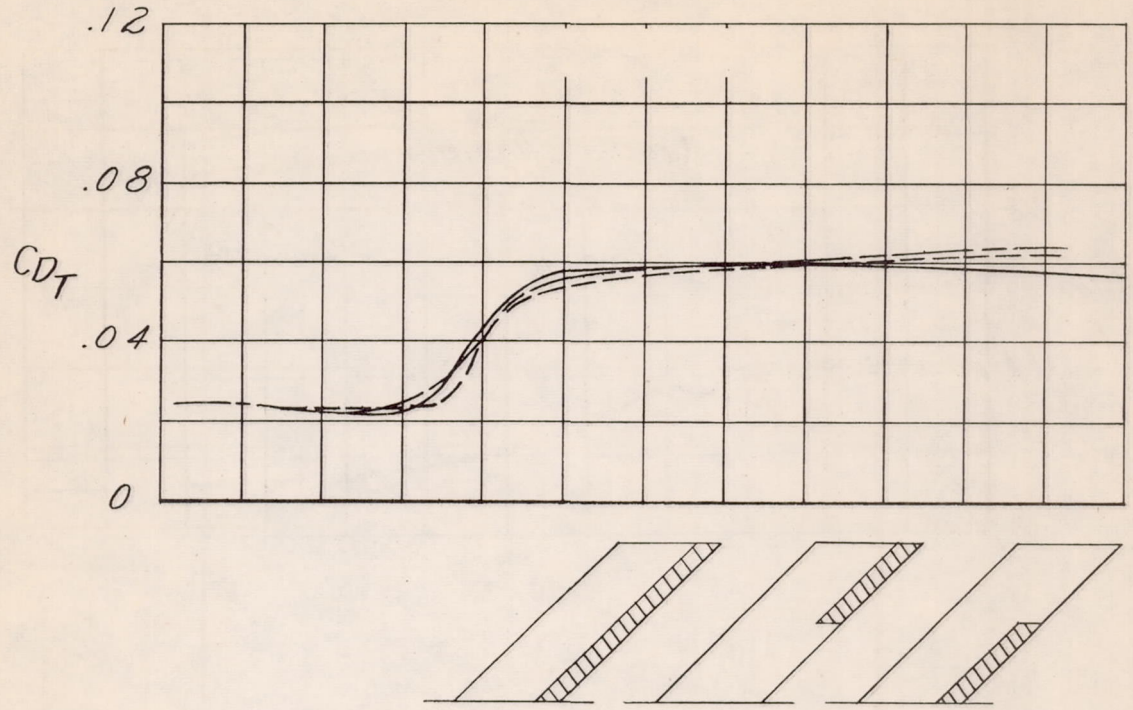

Calculated ($M \to 0$) ○ □ ◇

Experimental ——— - - - - - - ——— - - ———

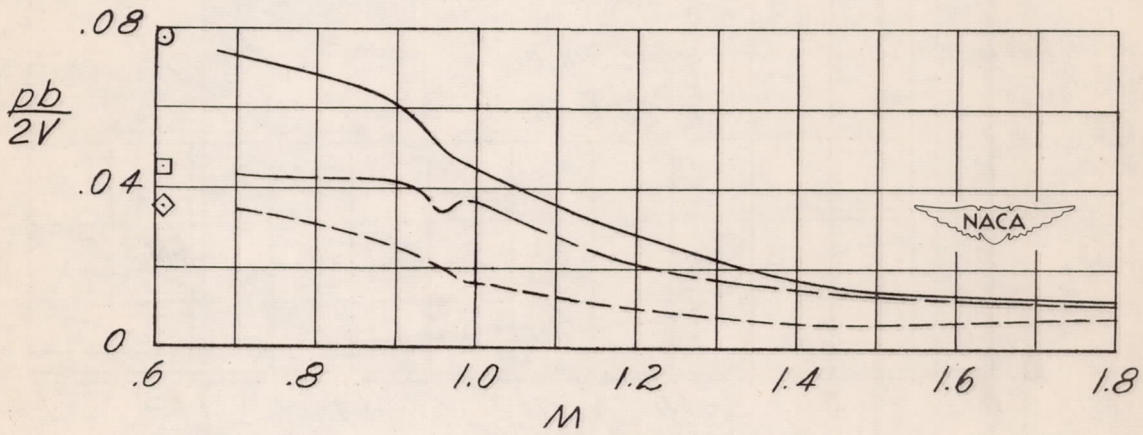

(b) $\Lambda = 45°$; $\delta_a = 5°$.

Figure 13.- Concluded.

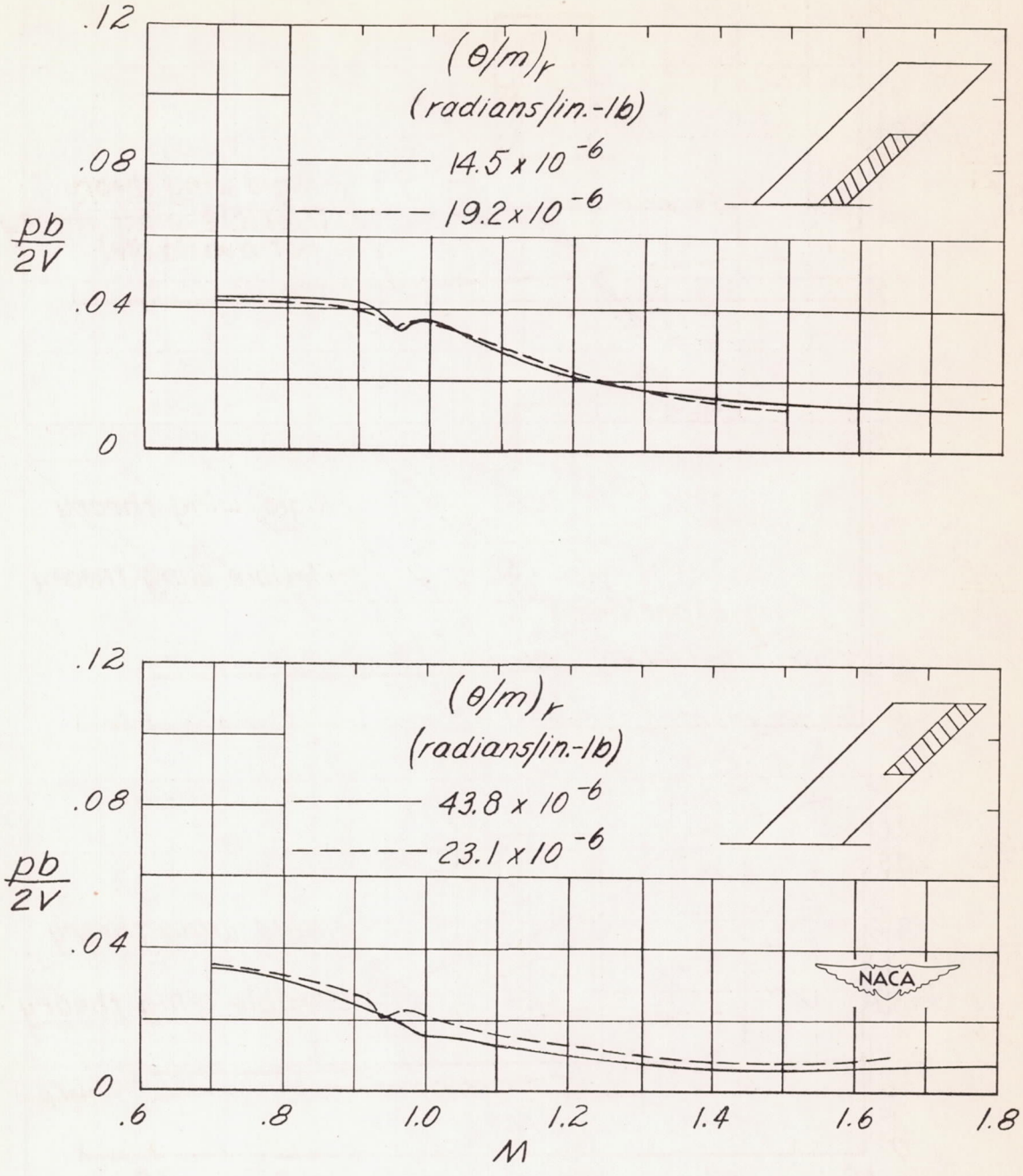

Figure 14.- Effect of change in torsional rigidity upon rolling effectiveness. Airfoil section 65A009; $\Lambda = 45°$; $A = 3.7$.

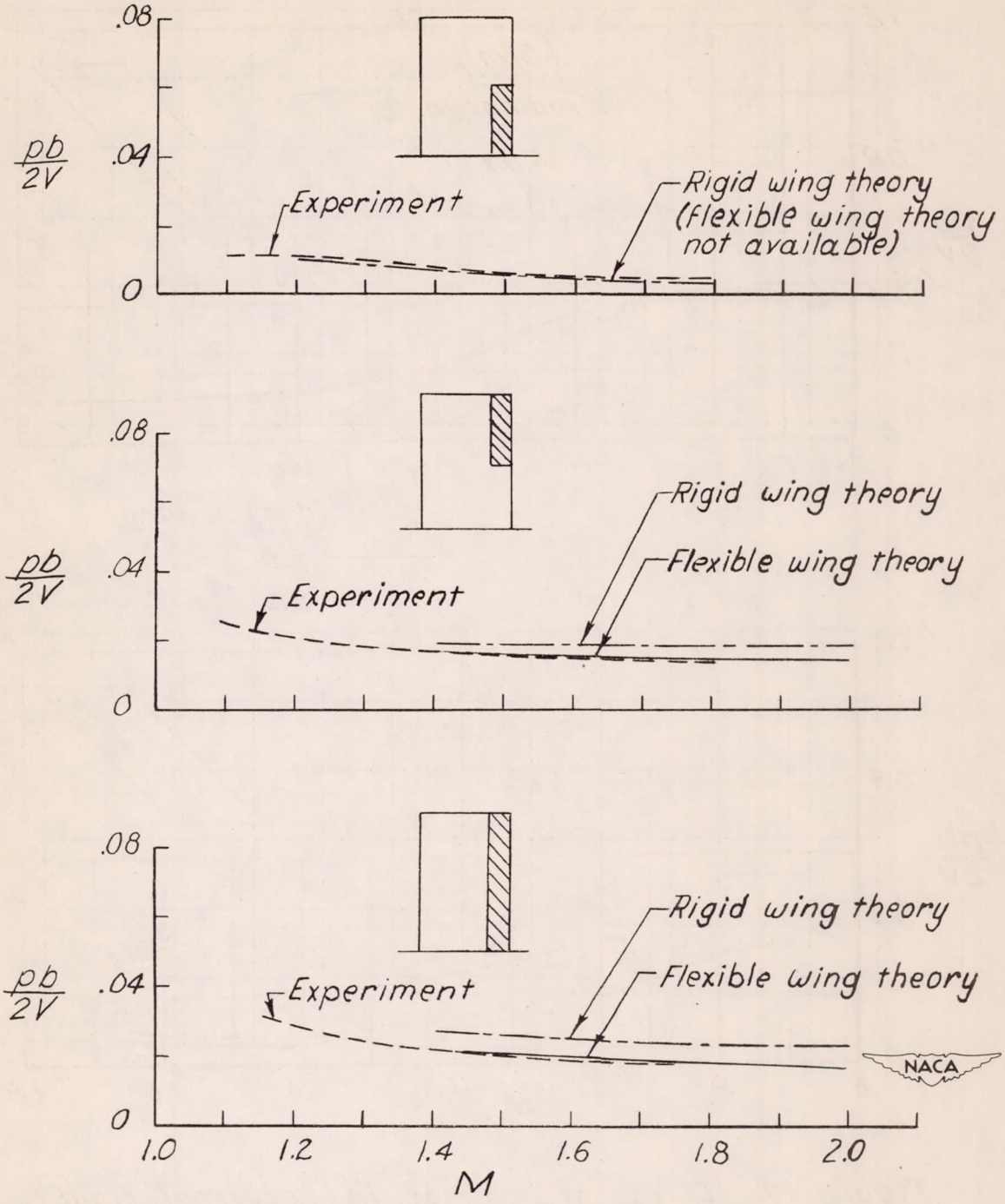

Figure 15.-Comparison of measured values with theory (refs. 5 and 6). $A = 3.7$; $\lambda = 1.0$; $\delta_a = 5°$.

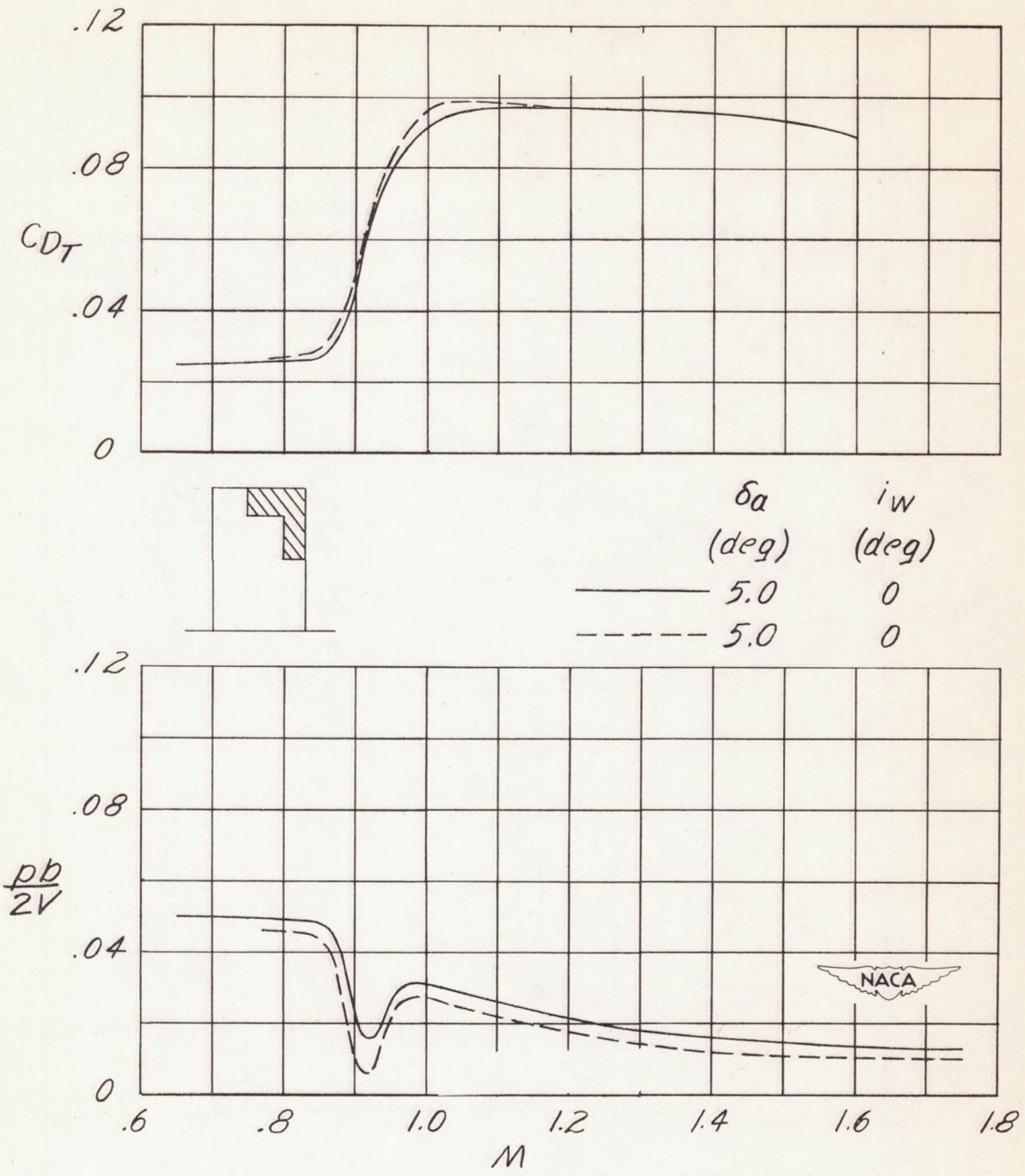

Figure 16.- Uncorrected flight data for outboard aileron with horn balance. Airfoil section 65A009; $\Lambda = 0°$; $A = 3.7$.

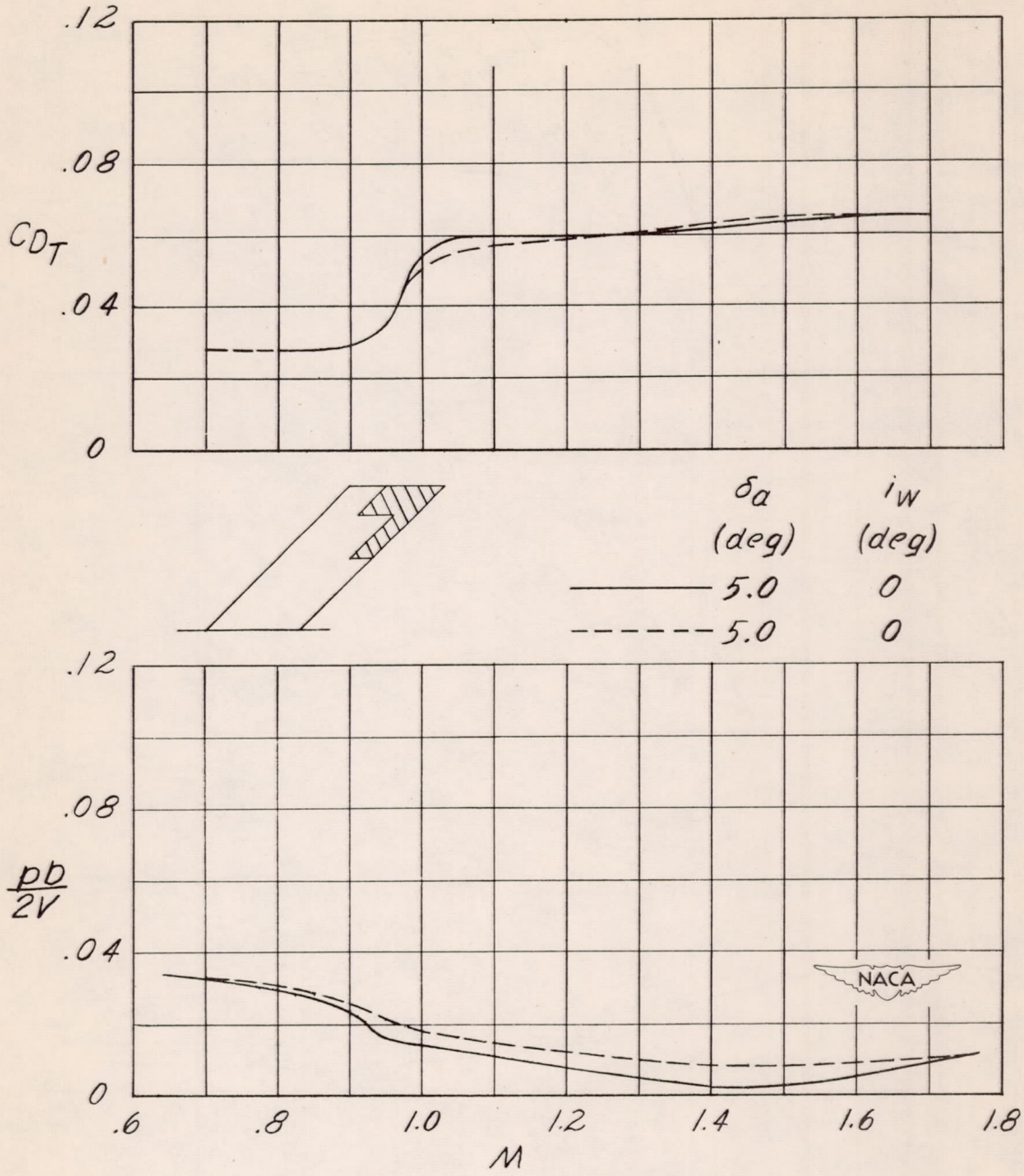

Figure 17.- Uncorrected flight data for outboard aileron with horn balance. Airfoil section 65A009; $\Lambda = 45°$; $A = 3.7$.

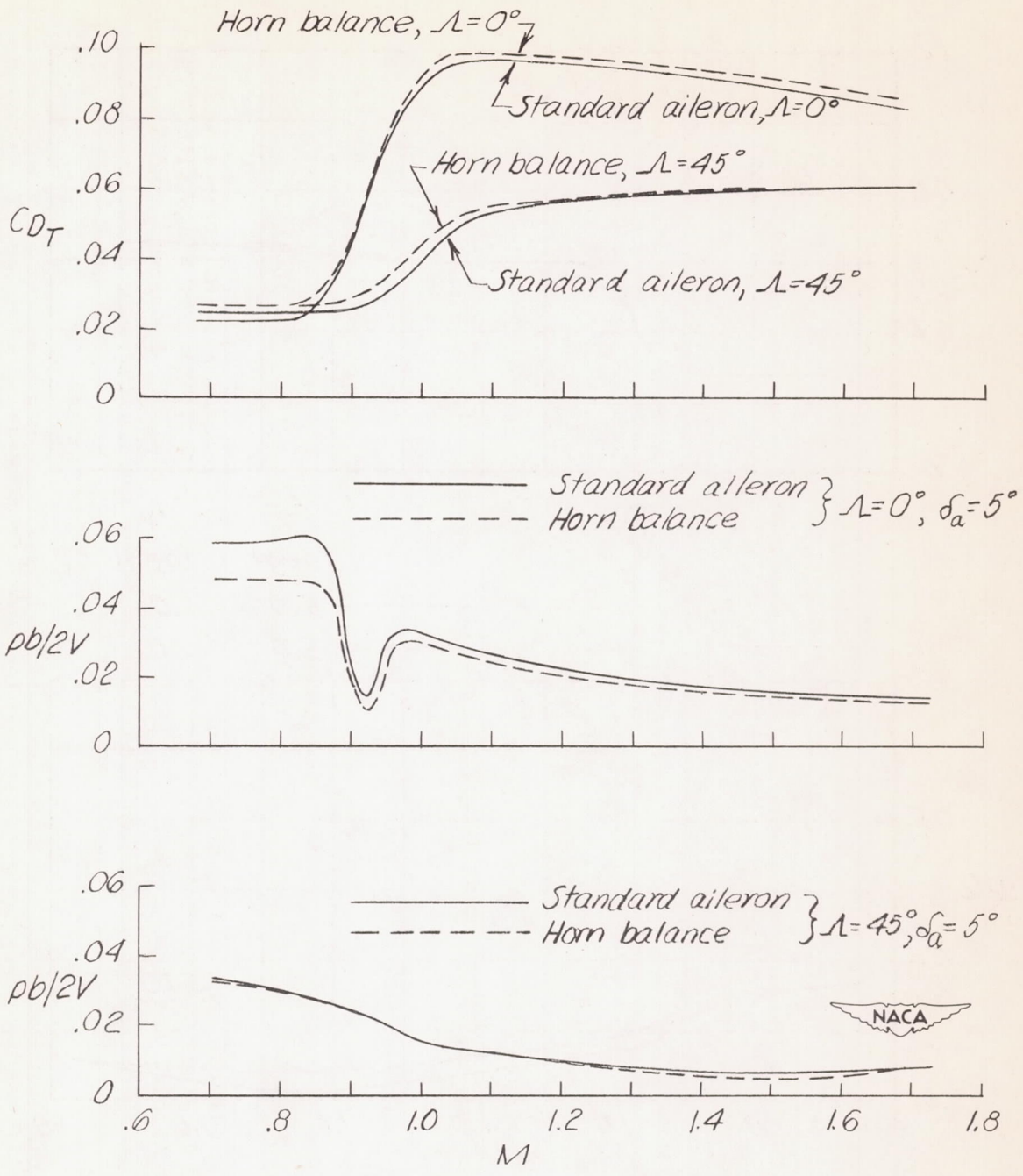

Figure 18.- Effect of a shielded horn balance on the variation of pb/2V and C_{D_T} with Mach number Airfoil section 65A009; λ = 1.0; A = 3.7.